DRAFT VERSION MARCH 11, 2010
Preprint typeset using LaTeX style emulateapj v. 08/22/09

ON STRONG MASS SEGREGATION AROUND A MASSIVE BLACK HOLE IMPLICATIONS FOR LOWER-FREQUENCY GRAVITATIONAL-WAVE ASTROPHYSICS

MIGUEL PRETO[1] & PAU AMARO-SEOANE[2]

(Dated: March 11, 2010)
Draft version March 11, 2010

ABSTRACT

We present, for the first time, a clear *N*-body realization of the *strong mass segregation* solution for the stellar distribution around a massive black hole. We compare our *N*-body results with those obtained by solving the orbit-averaged Fokker-Planck (FP) equation in energy space. The *N*-body segregation is slightly stronger than in the FP solution, but both confirm the *robustness* of the regime of strong segregation when the number fraction of heavy stars is a (realistically) small fraction of the total population. In view of recent observations revealing a dearth of giant stars in the sub-parsec region of the Milky Way, we show that the time scales associated with cusp re-growth are not longer than $(0.1-0.25)\times T_{rlx}(r_h)$. These time scales are shorter than a Hubble time for black holes masses $M_\bullet \lesssim 4\times10^6 M_\odot$ and we conclude that quasi-steady, mass segregated, stellar cusps may be common around MBHs in this mass range. Since EMRI rates scale as $M_\bullet^{-\alpha}$, with $\alpha\in[\frac{1}{4},1]$, a good fraction of these events should originate from strongly segregated stellar cusps.

Subject headings: black hole physics — galaxies: nuclei — stellar dynamics — gravitational waves

1. INTRODUCTION

The distribution of stars around a massive black hole (henceforth MBH) is a classical problem in stellar dynamics (Bahcall & Wolf 1976; Lightman & Shapiro 1977). The observational demonstration of the existence of nuclear stellar clusters (henceforth NSCs)—as revealed by a clear upturn in central surface brigthness—in the centers of galaxies makes its study ever more timely. A number of NSCs in coexistence with a central MBH have recently been detected (Graham & Spitler 2009) suggesting that NSCs around MBHs, like the one in the center of the Milky Way, may be quite common.

The renewed interest in this theoretical problem is thus motivated by the observational data in NSCs and, in particular, the very rich and detailed data available for the stars orbiting the Galactic MBH. At the same time, the prospects for detection of gravitational waves (GWs) from extreme mass ratio inspirals (henceforth EMRIs) with future GW detectors such as the *Laser Interferometer Space Antenna* (LISA) also urge us to build a solid theoretical understanding of sub-parsec structure of galactic nuclei. In fact, EMRI rates will depend strongly on the stellar density of compact remnants as well as on the detailed physics within $O(0.01\mathrm{pc})$ of the hole, which is the region from which these inspiralling sources are expected to originate (Hopman & Alexander 2005).

Bahcall & Wolf (1976) have shown, through a kinetic treatment that, in the case all stars are of the same mass, this quasi-steady distribution takes the form of power laws, $\rho(r)\sim r^{-\gamma}$, in physical space and $f(E)\sim E^p$ in energy space ($\gamma=7/4$ and $p=\gamma-3/2=1/4$). This is the so-called *zero-flow solution* for which the net flux of stars in energy space is precisely zero. Preto et al. (2004) and Baumgardt et al. (2004a) were the first to report *N*-body realizations of this solution, thereby validating the assumptions inherent to the Fokker-Planck (FP) approximation—namely, that scattering is dominated by uncorrelated, 2-body encounters and, in particular, dense stellar cusps populated with stars of the *same mass* are robust against ejection of stars from the cusp.

The properties of stellar systems that display a range of stellar masses are only very poorly reproduced by single mass models. It is well known from stellar dynamical theory that when several masses are present there is mass segregation—a process by which the heavy stars accumulate near the center while the lighter ones float outward (Spitzer 1987). Accordingly, stars with different mass get distributed with different density profiles. By assuming a stellar population with two mass components, Bahcall & Wolf (1977)—hencefort BW77—generalized their early cusp solution and argued heuristically for a scaling relation $p_L=m_L/m_H\times p_H$ that depends on the star's mass ratio only. However, they obtained no general result on the inner slope of the heavy objects; nor did they discuss the dependence of the result on the component's number fractions. On the other hand, it was shown long ago by Hénon (1969) that the presence of a mass spectrum leads to an increased rate of stellar ejections from the core of a globular cluster, but he did not include the presence of a MBH at the center. Hénon's work raises the question as to whether *multi-mass* stellar cusps, obtained from the solution of the FP equation, are robust against ejection of stars from the cusp. Ejections—due to strong encounters—are *a priori* excluded from the FP evolution, even though they could occur in a real nucleus. Furthermore, even if cusps were shown by *N*-body results to be robust against stellar ejections (and we show that they are in this Letter), BW77 scaling cannot be valid for arbitrary number fractions.

Recently Alexander & Hopman (2009)—henceforth AH09—stressed this latter point and have shown via FP calculations that, indeed, in the limit where the number fraction of heavy stars is realistically small, a new solution that they coined *strong mass segregation* obtains with density scaling as $\rho_H(r)\sim r^{-\alpha}$, where $\alpha\gtrsim2$. They have shown that there are two branches for the solution parametrized by

[1] (MP) Astronomisches Rechen-Institut, Zentrum für Astronomie, University of Heidelberg, D-69120 Heidelberg, Germany
[2] (PAS) Max Planck Intitut für Gravitationsphysik (Albert-Einstein-Institut), D-14476 Potsdam, Germany and Institut de Ciències de l'Espai, IEEC/CSIC, Campus UAB, Torre C-5, parells, 2na planta, ES-08193, Bellaterra, Barcelona, Spain

$\Delta = \frac{N_H M_H^2}{N_L M_L^2} \cdot \frac{4}{3+M_H/M_L}$. The *weak* branch, for $\Delta > 1$ corresponds to the scaling relations found by BW77; while the *strong* branch, for $\Delta < 1$, generalizes the BW77 solution. There is a straightforward physical interpretation. In the limit where heavy stars are very scarce, they barely interact with each other and instead sink to the center due to dynamical friction against the sea of light stars. Therefore, a quasi-steady state forms in which the heavy star's current is not nearly zero and thus the BW77 solution does not hold. As Δ increases, self-scattering of heavies becomes important and the resulting quasi-steady state forms with a nearly zero current for stars of all masses, so BW77 solution is recovered.

For all these reasons, it is fundamental to verify the Bahcall-Wolf solution—as well as its Alexander-Hopman generalization—with *N*-body integrations. There has been a surprisingly small number of *N*-body studies of multi-mass systems around a MBH (Baumgardt et al. 2004b; Freitag et al. 2006), and none of them reported the occurence of strong mass segregation.

In this Letter we use direct *N*-body integrations to show for the first time that: (i) strong mass segregation is a robust outcome of the growth of stellar cusps around a MBH when $\Delta < 1$; (ii) BW77 solution is recovered when $\Delta > 1$; (iii) as a corollary, we conclude that the rate of stellar ejections from the cusp is too low to destroy the high density cusps around MBHs—even though ejections from the cusp *do* occur. Furthermore, having validated the FP formalism, we proceed to use it to estimate the time scales for cusp re-growth starting from a wider range of models. Merritt (2009) obtained, for Milky Way type nucleus, times in large excess of a Hubble time. We use a FP formalism which, in contrast with that of the latter author, is tailored to follow the simultaneous evolution of the cusp of different stellar masses without any restrictions with respect to the values of $f(E)$ or $\rho(r)$. With our FP solutions we show that, for $M_\bullet \lesssim 5\times10^6 M_\odot$, the times for re-growing stellar cusps are shorter than a Hubble time. Our results clearly suggest that strongly segregated stellar cusps around MBHs in this mass range may be quite common in NSCs and should be taken into account when estimating EMRI event rates.

2. MODELS AND INITIAL CONDITIONS

We have performed the *N*-body simulations with a modified version of *NBODY4* (Aarseth 1999, 2003) adapted to the *GRAPE* − 6 special-purpose hardware. The code was modified to add the capture of stars by the MBH: stars that enter a critical radius r_{cap} from the hole are captured and their mass is added to the hole. The new position and velocity of the new massive particle are calculated by imposing that the capture process conserves total linear momentum. The maximum number of particles supported by the memory of a micro-GRAPE board is $\sim 1.2\times10^5$, which have been shown to be sufficient to accurately describe the evolution of the bulk properties (densities in physical and phase space) of the nuclear stellar cluster (Preto et al. 2004), but is not enough to resolve its loss cone dynamics accurately. Therefore, we do not attempt a detailed modelling of tidal disruption processes and set the capture radius to be equal for all particles. The MBH dominates the dynamics inside its influence radius r_h defined to be the radius which encloses twice of its mass at $t = 0$. The stellar distribution evolves and reaches its asymptotic quasi-steady state over relaxation time scales (Spitzer 1987):

$$T_{rlx}(r_h) \sim 0.34 \frac{\sigma_h^3}{G^2 \rho_h m_* \ln\Lambda}, \qquad (1)$$

where σ_h and ρ_h are, respectively, the $1D$ velocity dispersion and spatial density evaluated at r_h. Following Preto et al. (2004), we define the Coulomb logarithm $\ln\Lambda = \ln(r_h\sigma_h^2/2Gm_*)$.

Runs	γ	$M_\bullet/M_g$	f	Δ	r_h	$\ln\Lambda$
6	1	0.05	2.5×10^{-3}	0.08	0.46	8.3
6	1	0.05	$5.\times10^{-3}$	0.15	0.46	8.3
6	1	0.05	7.5×10^{-3}	0.23	0.46	8.3
6	1	0.05	0.01	0.31	0.46	8.3
4	1	0.05	0.429	13.2	0.46	8.3
2	1/2	0.01	2.5×10^{-3}	0.08	0.26	7.2
2	1/2	0.01	$5.\times10^{-3}$	0.15	0.26	7.2
2	1/2	0.01	7.5×10^{-3}	0.23	0.26	7.2
2	1/2	0.01	0.01	0.31	0.26	7.2

TABLE 1
N-BODY INTEGRATIONS. 1st COLUMN: NUMBER OF RUNS; 2nd COLUMN: SLOPE OF THE DEHNEN'S MODEL INNER CUSP AT $t = 0$; 3rd: RATIO OF BH MASS TO TOTAL CLUSTER MASS IN STARS; 4th: $f = N_H/N$ FRACTION OF HEAVY MASS PARTICLES; 5th: ALEXANDER & HOPMAN PARAMETER; 6th: INFLUENCE RADIUS r_h; 7th: COULOMB LOGARITHM AT r_h. THE TOTAL NUMBER OF PARTICLES IS $N = 1.24\times10^5$ IN ALL RUNS; THE MASS RATIO BETWEEN HEAVY AND LIGHT COMPONENTS IS $R = 10$ FOR ALL RUNS. THE TIDAL CAPTURE RADIUS $r_{cap} = 10^{-7}$ IN ALL RUNS. WE USE UNITS $G = M_{nuc} = a = 1$, WHERE M_{nuc} IS THE TOTAL MASS OF THE NUCLEAR CLUSTER AND a IS THE DEHNEN MODEL'S SCALE LENGTH.

A realistic mass population of stars with a continuous range of stellar masses can be approximately represented by two (well-separated) mass scales: one in the range $\mathcal{O}(1M_\odot)$ corresponding to low mass main-sequence stars, white dwarfs (WDs) and neutron stars (NSs); another with $\mathcal{O}(10M_\odot)$ representing stellar black holes (SBHs). The relative abundance of objects in these mass ranges is overwhelmingly dominated by the lighter stars — typical number ractions of SBHs being of $\mathcal{O}(10^{-3})$ (Alexander 2005). The initial stellar model is built from a Dehnen model of a spherical galaxy (Dehnen 1993) to which a massive particle is added at the center at rest (Tremaine et al. 1994). The positions and velocities are Monte-Carlo realizations that accurately reproduce the spatial $\rho(r)$ and phase space $f(E)$ densities with stars of the same mass. In order to generate a two-component model, we proceed as follows: (1) we specify the mass ratio $R = m_H/m_L$ between heavy and light stars, and respective number fractions $f_H = N_H/N$ and $f_L = 1 - f_H$, through which the AH09 Δ parameter is fixed; (2) we assign the mass m_H or m_L randomly to each star according to the statistical weights f_H and f_L, respectively. The resulting model is almost in dynamical equilibrium; deviations of virial ratio from unity are $\lesssim 1-2\%$. On a dynamical time scale, phase mixing occurs and the virial ratio converges to unity to within a fraction of a percent. Following this prescription, the two-component models start without any mass segregation, as would be expected from a violently relaxed system. Dehnen model's density has $\rho(r) \propto r^{-\gamma}$ at the center and the corresponding distribution function $f(E)$ is isotropic. Table 1 gives the list of runs and adopted parameters.

3. FOKKER-PLANCK MODELS FOR SEVERAL STELLAR MASSES

We also study the evolution of the NSC with a multi-mass Fokker-Planck formalism and compare results with the *N*-body integrations. The time-dependent, orbit-averaged,

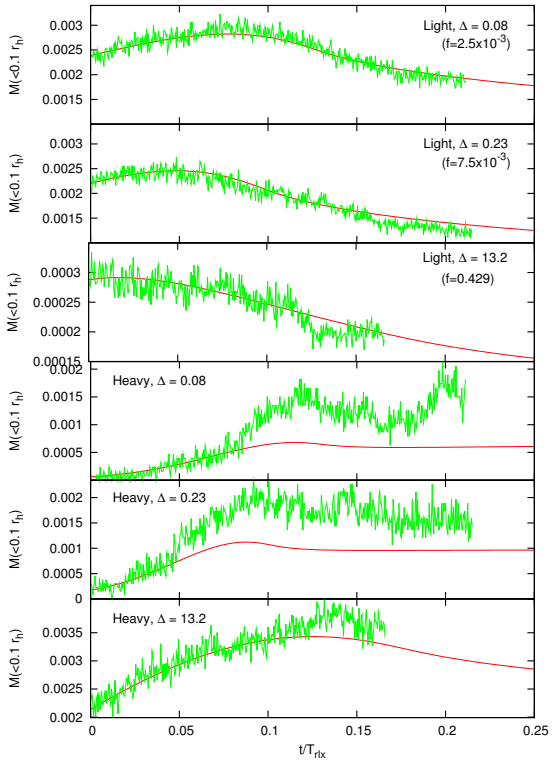

FIG. 1.— Evolution of stellar mass within $0.1\,r_h$ from the MBH, for light (3 upper panels) and heavy (3 lower panels) components. Noisy curves are from N-body integrations; smooth curves are from the Fokker-Planck evolution.

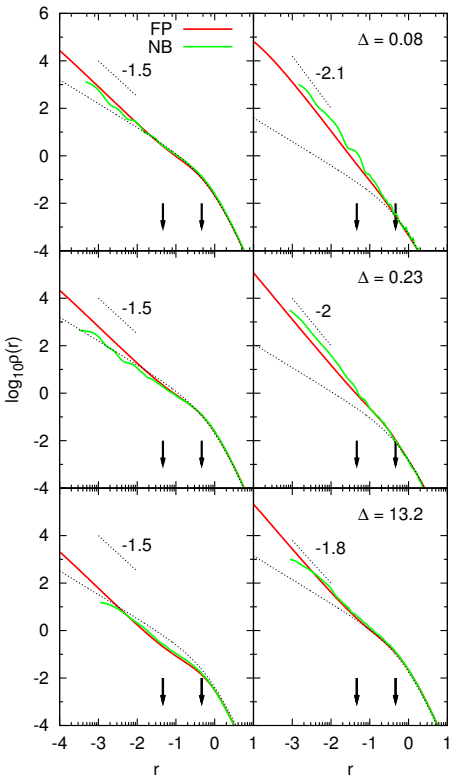

FIG. 2.— The mass density profiles around the MBHs for both components at the end of the integrations. N-body and Fokker-Planck curves are superimposed for comparison. Left panels show $\rho_L(r)$ for the light component; right panels show $\rho_H(r)$ for heavy component. The arrows signal the location of $0.1r_h$ and r_h radii. These plots highlight the asymptotic solution of both methods is in good agreement and $\rho_H \sim r^{-\gamma_H}$, where γ_H decreases from values $\gtrsim 2$ down to $\sim 7/4$ while moving from the strong to the weak branch of the solution.

isotropic, Fokker-Planck equation in energy space is defined, for each component (Spitzer 1987; Chernoff & Weinberg 1990), by

$$p(E)\frac{\partial f_i}{\partial t} = -\frac{\partial F_{E,i}}{\partial E},\; F_{E,i} = -D_{EE,i}\frac{\partial f_i}{\partial E} - D_E f_i, \qquad (2)$$

$$D_{EE,i} = 4\pi^2 G^2 m_*^2 \mu_i^2 \ln\Lambda \times \sum_j^{N_c}\left[\left(\frac{\mu_j}{\mu_i}\right)^2 q(E)\int_{-\infty}^{E} dE'\, f_j(E') + \int_E^{+\infty} dE' q(E') f_j(E')\right], \qquad (3)$$

$$D_{E,i} = -\sum_j^{N_c}\left(\frac{\mu_j}{\mu_i}\right)\int_E^{+\infty} dE' p(E') f_j(E'). \qquad (4)$$

In this equation, i, j run from 1 to N_c (the number of mass components), $\mu_i = m_i/m_*$ where $m_* = 1/N$ is a reference mass. $p(E) = 4\int_0^{r_{max}(E)} dr\; r^2\sqrt{2(E-\Phi(r))} = -\partial q/\partial E$ is the phase-space accessible to each (bound) star of specific energy $E = -v^2/2 + \Phi(r) > 0$ (Spitzer 1987), and the total gravitational potential $\Phi(r)$ is the sum of the contribution from the nuclear cluster plus the hole. During our simulations, the stellar distribution and its resulting gravitational potential change substantially inside r_h only—the region over which the MBH's potential is dominant—so we keep the contribution from the stars to total $\Phi(r)$ fixed throughout. This system of FP equations treats self-consistently both dynamical friction and two-body scattering between all components, without any further approximations other than those inherent to the FP formalism. In contrast with Merritt (2009), our treatment is not limited to early evolution where the heavy component is just a small perturbation on the (time evolving and dominant in number) light component. As a result, we can follow both weak and strong branches of the solution throughout without restriction. We solve the FP equations (2, 3) using the Chang & Cooper (1970) integration scheme.

4. RESULTS

The density of stars around the MBH increases as the cusp grows for both light and heavy components until it reaches a quasi-steady state; afterwards, the lights start to slowly expand. This can be seen in Figure 1, where the mass inside a sphere of $0.1r_h$, centered on the MBH, is depicted as a function of time. This distance is measured with respect to the *instantaneous* position of the MBH. Both curves from FP and NB are shown together for three different runs with $\Delta = 0.08, 0.23$ corresponding to strong segregation and $\Delta = 13.2$ to weak segregation branches. The time scaling between NB and FP is related through $T_{rlx}^{FP} = \ln\Lambda/N\; T_{rlx}^{NB}$, and no further adjustements were made. In the three cases shown (as in all others cases tested but not shown), the agreement between both methods is very good, although there is a noticeable tendency for the heavy particles in the NB runs to segregate more strongly in the central cusp—this is especially the case in the strong branch. Figure 1 also suggests that a quasi-steady state (and maximum central concentration) have been reached by the end of the runs correspond-

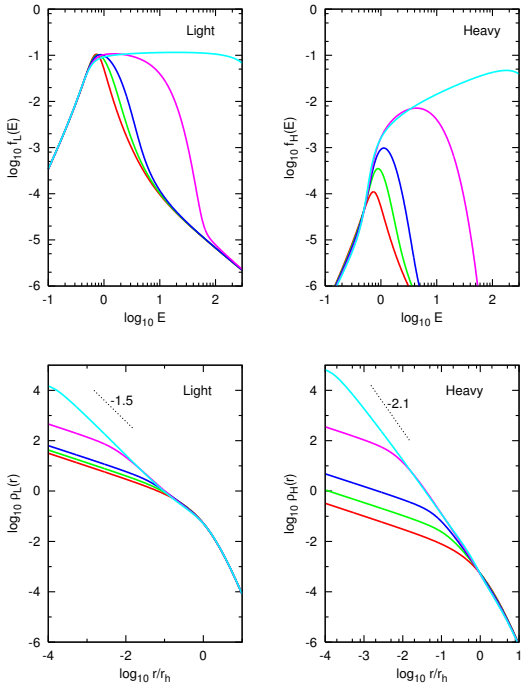

FIG. 3.— Evolution of the phase space density (upper panels) and spatial density (lower panels) for both components. The models starts with $\gamma = 1/2$, purported to represent a cored nuclei; the fraction of stellar black holes is $f = 10^{-3}$ and their mass is 10 times larger than that of the light stars. Both densities increase monotonically with time and are shown at $t/T_{rlx} = 0, 0.05, 0.1, 0.2, 0.25$.

ing to $t \sim (0.1-0.2)T_{rlx}(r_h)$. We stress that mass segregation, whether in the weak or strong branch, speeds up cusp growth by factors ranging from 4 to 10 in comparison with the single-mass case (Preto et al. 2004).

Figure 2 displays the spatial density profiles $\rho_L(r)$ and $\rho_H(r)$ at late times, $t \sim 0.2T_{rlx}(r_h)$. The agreement between both methods is again quite good although there is the tendency, in the strong branch, for NB's asymptotic slope γ_L to be slightly smaller than in FP—for which $\gamma_{L,min} = 1.5$. The slopes of the inner density profiles of the heavy component decrease as the solution evolves from the strong to the weak branch when Δ is increased, as expected. In the limit of $\Delta >> 1$, γ_H tends to evolve to a quasi-steady state close to the $7/4$ solution, while for $\Delta << 1$, $\gamma_H \gtrsim 2$. The asymptotic inner density slopes, in both solution branches, of the light component extend out to $\sim 0.1r_h$; in contrast, the heavy component shows a different behavior depending on the solution branch: on the weak branch, γ_H's asymptotic slope also extends only up to $\sim 0.1r_h$, while on the strong branch it extends virtually all the way to r_h. In the strong branch, the density of the heavy component exceeds that of the light for $r \lesssim 0.01r_h$ (and will therefore dominate the interaction events with the MBH); in the strong branch, $\rho_H > \rho_L$ throughout.

Although there are some differences in quantitative detail, these NB results broadly confirm the FP calculations and validate its inherent assumptions—at least in what concerns the description of the *bulk* properties of stellar distributions. A more detailed study and description of the stellar dynamics around a MBH under different initial conditions and different

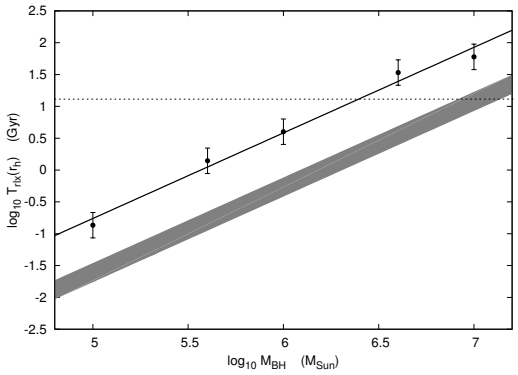

FIG. 4.— The points represent the relaxation time at the influence radius r_h for single mass, cored models of NSCs as a function of MBH mass. The shaded area covers the region $[0.1T_{rlx}, 0.2T_{rlx}]$, which is time for cusp re-growth computed with the Fokker-Planck equation. Its finite width results from the distribution of parameters: the number fraction of stellar BHs $f \in [10^{-3}, 10^{-2}]$ and mass ratio $R = 10, 15, 20$. The horizontal curve (with points) corresponds to a Hubble time 13 Gyr. NSCs with MBH masses below that of *SgrA** can re-grow their stellar cusps after $\lesssim 6$ Gyr.

models (allowing for more than the two components reported here), stellar ejections (which *do* occur in the NB runs) and captures, and further comparisons between NB and FP methods, are outside the scope of this Letter and are the subject of another work in preparation.

5. IMPLICATION FOR GALACTIC NUCLEI AND SOURCES OF GWS

The analysis of the number counts of spectroscopically identified, old stars in the sub-parsec region of our own Milky Way (Buchholz et al. 2009; Do et al. 2009)—believed to be complete down to magnitude $K = 15.5$—reveals a deficit of old stars with respect to the high number a strongly segregated cusp would entail. Although the slope of the density profile is still weakly constrained, the best fits from number counts data seem to exclude with certainty slopes $\gamma > 1$ (Schödel et al. 2009), and there could be a core with a stellar density decreasing towards the center, $\gamma < 0$, although such a fit is only marginally better than one with $\gamma \sim 1/2$.

Although we deem to be too early to conclude for the inexistence of a segregated cusp around *SgrA**, since the detectable stars (essentially giants) are still a small fraction of the stellar population as a whole, we next compute the time necessary for cusp growth if at some point a central core is carved in the stellar distribution. Having validated the FP approach and its results we study equations (2, 3), which are orders of magnitude faster to solve than NB integrations.

We choose as initial condition a model with $\gamma = 1/2$ (which is the minimum slope that allows an isotropic solution around a MBH), since the isotropization time—the time necessary for the establishment of this shallow cusp starting from a hole in the spatial distribution—is $\ll T_{rlx}(r_h)$ (Merritt 2009), and we are interested in the evolution over $O(T_{rlx})$ time scales. Figure 3 shows the evolving phase-space $f(E)$ and spatial $\rho(r)$ densities for both components ($R = 10$ and $f = 0.001$ constitute our fiducial case). It can be seen that, by $t \sim 0.25\ T_{rlx}(r_h)$, cusps with $\gamma_L \sim 1.5$ and $\gamma_H \sim 2$ (or $p_L \sim 0.05$ and $p_H \sim 0.5$ in phase space) are fully developed; a little earlier, at $t \sim 0.2\ T_{rlx}(r_h)$, the density cusp $\rho_H(r)$ is already fully developed down to $r \sim 0.01r_h$ (~ 0.02 pc if scaled to the Milky Way nucleus). If there was some event carving a hole in the stellar distribution around *SgrA** more than 6 Gyr ago, then there

was enough time for a very steep cusp of stellar BHs to have re-grown.

The number fraction f of SBHs is sensitive to the initial mass function (IMF) of high mass stars. There are indications the IMF in galactic nuclei is top-heavy (Maness et al. 2007) so we adopt a range of values $f \in [10^{-3}, 10^{-2}]$; the mass distribution of SBHs is also weakly constrained so we follow O'Leary et al. (2009) in considering several mass ratios $R = 10, 15$ and 20. Figure 4 shows the relaxation times at the influence radius for nuclei with MBH masses in the range of interest for LISA; the straight line is a linear fit to the points. The shaded region corresponds to the range $[0.1\ T_{rlx}(r_h), 0.2\ T_{rlx}(r_h)]$ and represents the time stellar cusps take to grow starting from an isotropic core. The shaded region's width results from the distribution of values for R and f. In the ranges we adopted, increasing R or f both have the effect of decreasing the time for cusp growth. At early times, SBHs essentially evolve under dynamical friction with characteristic time scale $T_{df} \sim T_{rlx}/R$; increasing f leads to an increased rate of self-scattering between SBHs at late times.

6. SUMMARY AND DISCUSSION

Our results show that strong mass segregation is a *robust* outcome from the growth of stellar cusps around MBHs. We have used N-body integrations with two masses—light and heavy components representing main sequence stars and stellar BHs respectively—, and compared the results with those obtained with the FP formalism. The broad agreement between both methods validates the FP description of the *bulk* properties of time-evolving stellar distribution around a MBH—and its underlying assumptions. The differences of quantitative detail are the subject of another work in preparation.

Using the FP equation to study cusp growth under a variety of initial conditions purported to represent cored nuclei, we have shown that the time scales associated with cusp regrowth are clearly shorter than a Hubble time for nuclei with MBHs in the mass range $M_\bullet \lesssim 5 \times 10^6 M_\odot$—even though the relaxation time, as estimated for a single mass stellar distribution, exceeds a Hubble time in the upper part of this mass range. Therefore, our work strongly suggests that quasi-steady—strongly segregated— stellar cusps may be common around MBHs with masses in this range.

EMRIs of compact remnants will be detectable by LISA precisely for MBHs in this mass range (de Freitas Pacheco et al. 2006; Amaro-Seoane et al. 2007; Babak et al. 2007). Estimates for event and detection rates by LISA costumarily assume that the stellar cusps are in steady state (Hopman & Alexander 2006a,b). But recent observations reveal a dearth of giants inside 1 pc from $SgrA^*$ and raise the possibility that cored nuclei are common—this scenario has been thoroughly explored by Merritt (2009).

Our results strongly suggest that stellar cusps can re-grow in less than a Hubble time. The existence of cored nuclei still remains plausible though—especially for nuclei with MBHs in the upper part of the mass range—, since time scales are still quite long (*e.g.* 6 Gyr in Milky Way type nuclei). However, since EMRI rates scale as $M_\bullet^{-\alpha}$, $\alpha \in [\frac{1}{4}, 1]$, and regrowth times are $\lesssim 1$ Gyr for $M_\bullet \lesssim 1.2 \times 10^6 M_\odot$, we still expect that a substantial fraction of EMRI events will originate from segregated stellar cusps. Finally, indirect observations alone will reveal whether there is a "hidden" cusp of old stars and their dark remnants around $SgrA^*$ (Weinberg et al. 2005; Preto & Saha 2009).

MP and PAS acknowledge support by DLR (Deutsches Zentrum für Luft- und Raumfahrt). The simulations have been carried out on the dedicated high-performance GRAPE-6A clusters at the Astronomisches Rechen-Institut in Heidelberg; [3] some of the simulations were done at the TUFFSTEIN cluster of the AEI.

[3] GRACE: see http://www.ari.uni-heidelberg.de/grace

REFERENCES

Aarseth, S. J. 1999, PASP, 111, 1333
—. 2003, Gravitational N-Body Simulations (Cambridge, UK: Cambridge University Press, November 2003.)
Alexander, T. 2005, Phys. Rep., 419, 65
Alexander, T. & Hopman, C. 2009, ApJ, 697, 1861
Amaro-Seoane, P., Gair, J. R., Freitag, M., Miller, M. C., Mandel, I., Cutler, C. J., & Babak, S. 2007, Classical and Quantum Gravity, 17, 113
Babak, S., Fang, H., Gair, J. R., Glampedakis, K., & Hughes, S. A. 2007, Phys. Rev. D, 75, 024005
Bahcall, J. & Wolf, R. 1976, ApJ, 209, 214
—. 1977, ApJ, 216, 883
Baumgardt, H., Makino, J., & Ebisuzaki, T. 2004a, ApJ, 613, 1133
—. 2004b, ApJ, 613, 1143
Buchholz, R., Schödel, R., & Eckart, A. 2009, A&A, 499, 483
Chang, J. & Cooper, G. 1970, J. Comput. Phys., 6
Chernoff, D. F. & Weinberg, M. D. 1990, ApJ, 351, 121
Dehnen, W. 1993, MNRAS, 265, 250
Do, T., Ghez, A. M., Morris, M. R., Lu, J. R., Matthews, Keith andYelda, S., & Larkin, J. 2009, ApJ, 703, 1323
Freitag, M., Amaro-Seoane, P., & Kalogera, V. 2006, ApJ, 649, 91
de Freitas Pacheco, J.A., Filloux, C., & Regimbau, T. 2006, Phys. Rev. D, 74, 023001
Graham, A. W. & Spitler, L. R. 2009, MNRAS, 397, 2148
Hénon, M. 1969, A&A, 2, 151
Hopman, C. 2009, Classical and Quantum Gravity, 26, 094028
Hopman, C. & Alexander, T. 2005, ApJ, 629, 362
Hopman, C. & Alexander, T. 2006a, ApJ, 645, 1152
—. 2006b, ApJ, 645, 133
Lightman, A. P. & Shapiro, S. L. 1977, ApJ, 211, 244
Maness, H., Martins, F. andTrippe, S., Genzel, R., Graham, J. R., Sheehy, C., Salaris, M., Gillessen, S., Alexander, T., Paumard, T., Ott, T., Abuter, R., & Eisenhauer, F. 2007, ApJ, 669, 1024
Merritt, D. 2009, arXiv:0909.1318
O'Leary, R., Kocsis, B., & Loeb, A. 2009, MNRAS, 395, 2127
Preto, M., Merritt, D., & Spurzem, R. 2004, ApJ, 613, L109
Preto, M. & Saha, P. 2009, ApJ, 703, 1743
Schödel, R., Merritt, D., & Eckart, A. 2009, A&A, 502, 91
Spitzer, L. 1987, Dynamical evolution of globular clusters (Princeton, NJ, Princeton University Press, 1987, 191 p.)
Tremaine, S., Richstone, D. O., Byun, Y.-I., Dressler, A., Faber, S. M., Grillmair, C., Kormendy, J., & Lauer, T. R. 1994, AJ, 107, 634
Weinberg, N. N., Milosavljević, M., & Ghez, A. M. 2005, ApJ, 622, 878